WARSAW UNIVERSITY OF TECHNOLOGY Index 351733
FACULTY OF CIVIL ENGINEERING
COMMITTEE FOR CIVIL AND WATER ENGINEERING
POLISH ACADEMY OF SCIENCES ISSN 1230-2945

DOI: 10.24425/ace.2025.156170

ARCHIVES OF CIVIL ENGINEERING

Vol. LXXI ISSUE 4 2025



**pp. 283 –298**



**Research paper**

# Damage characteristics analysis of self-anchored suspension bridge

**Xilong Zheng[1], Yunfeng Hu[2], Baitao Sun[3]**

**Abstract:** Based on a self-anchored suspension bridge with a long span and complex structure, this paper makes a detailed analysis of its stress characteristics before damage and damage characteristics after damage through finite element analysis and bridge load test. Aiming at the main vulnerable components of the main girder, a variety of identification methods based on the existing dynamic damage identification methods are selected for comparative analysis of damage identification, and finally an effective method suitable for bridge girder damage monitoring is determined according to the identification effect of each method. Different damages of main girder, bridge tower and suspender are simulated respectively, and then the static and dynamic damage characteristics of the structure under the same conditions before and after the damage are analyzed with the results of nondestructive analysis of the bridge as reference. The results show that the internal force and deformation caused by the same static and dynamic load and the inherent dynamic characteristics of the structure will change correspondingly when different damages occur to the structure, but the change is small for the moderate damage of 20%. After the suspenders fail completely, the deformation and internal force of the bridge will increase greatly, and the cable force of the adjacent suspenders will increase by 50%.

**Keywords:** self-anchored suspension bridge, damage characteristics, cable damage, monofilament

[1]PhD., Key Laboratory of Earthquake Engineering and Engineering Vibration, Institute of Engineering Mechanics, China Earthquake Administration, No.29 Xuefu Road, Harbin, China, e-mail: zhengxilong88@163.com, ORCID: 0009-0001-7945-1562

[2]MSc., Engineering Department, Ningbo Traffic Engineering Construction Group Co., LTD, No. 3388 Canghai Road, Ningbo, China, e-mail: yunfenghu1981@163.com, ORCID: 0009-0001-2509-5910

[3]Prof., Key Laboratory of Earthquake Engineering and Engineering Vibration, Institute of Engineering Mechanics, China Earthquake Administration, No.29 Xuefu Road, Harbin, China, e-mail: sunbt@iem.ac.cn, ORCID: 0009-0002-2548-194X

# 1. Introduction

From the construction history, self-anchored suspension bridge is not a new bridge type, which can be traced back to the 19th century at the earliest. Until 1990s, due to the perfection of calculation theory and the breakthrough of computer-aided design, self-anchored suspension bridges ushered in real development [1]. With the advantages of novel structure, beautiful appearance, reasonable span arrangement and no anchorage, self-anchored suspension bridge has become a competitive bridge type in the city and has been developed and applied more at home and abroad. Structural damage identification technology was first put forward in 1950s, which originated from the fault diagnosis of dynamic structures, and it is a multidisciplinary comprehensive subject [2, 3]. With the rapid development of the military industry, damage identification technology has been paid great attention by governments all over the world, and has gone through three important development stages [4–6].

The damage identification methods can be roughly divided into two categories: damage identification based on static response and damage identification based on dynamic characteristics [7]. Among them, the former is mainly based on the measured changes of static parameters such as deformation and strain related to the performance of the bridge structure [8, 9]. The latter is based on the change of structural dynamic parameters as a means of structural damage identification. In the research of damage identification based on structural dynamic characteristics, the natural frequency, damping, modal shape and acceleration frequency response function of the structure are mainly selected as damage identification parameters to judge the location and degree of structural damage [10–12].

Considering that damage identification technology, whether through structural static or structural dynamic characteristics, mainly relies on structural physical model for damage diagnosis, sometimes there are problems such as complex and huge calculation model and difficulty in modeling large-scale structures [13–15]. Due to the problems of measurement noise, uncertainty of environmental conditions and incomplete measurement data, there are still some problems in the practical application of damage diagnosis method based on structural testing, which need further exploration and improvement [16–18].

In this paper, the structural response before and after the damage and the applicability of the damage identification method of the main girder are studied mainly by finite element software simulation. The damage treatment of finite element model is used to simulate the damage state of the main components of the bridge, such as main girder, pylon and suspender. Through the static and dynamic comparative calculation of the self-anchored suspension bridge before and after the damage, the influence of the damaged components on the static and dynamic characteristics of the bridge is analyzed, and the corresponding structural damage characteristics are found out. Select the appropriate dynamic or static damage identification index, compare and analyze the damage identification effect of the main girder, and determine the effective method suitable for the main girder damage of the self-anchored suspension bridge.

# 2. Project overview

A bridge is a self-anchor suspension bridge with five-tower steel-concrete composite beam. The span layout is 108 m + 248 m + 108 m, the main span ratio is 1/2.3, and the vertical span ratio of the main span is 1/5. The whole bridge facade is shown in Fig. 1. The design load is highway I. The net width of bridge deck: 2.0 m (side walk) +15.5 m (road way) +2.0 m (middle belt) +15.5 m (road way) +2.0 m (side walk). The calculated driving speed is 80 km/h.

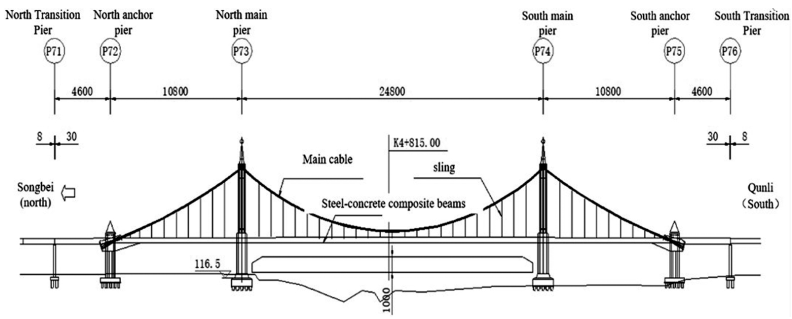


Fig. 1. Elevation view of bridge (unit: cm)

(1) Bridge tower

The bridge tower is a reinforced concrete H-type structure, the concrete grade is C50, the main height of the bridge tower is 80.5 m, and the tower column section is box type. The tower column is divided into three sections. The section size of the upper tower column is 5.4 m (vertical) × 3.1 m (horizontal), the short wall thickness is 70 cm and the long wall thickness is 55 cm. The section size of the middle tower column is 6.0 m (vertical) × 3.4 m (horizontal), short wall thickness 110 cm and long wall thickness 95 cm. The section size of the lower tower column is 8.0 m (vertical) × 4.4 m (horizontal).

(2) Stiffened beam

The main span and side span stiffened beam adopts steel-concrete composite beam. The composite beam is composed of the steel bridge deck system composed of steel main beam, beam and small longitudinal beam to form the overall composite section. The cross section is shown in Fig. 2. The main beam height is 3.2 m (height inside the outer web), the wide (width inside the web) is 2.1 m. The full width of the bridge deck is 40 m.

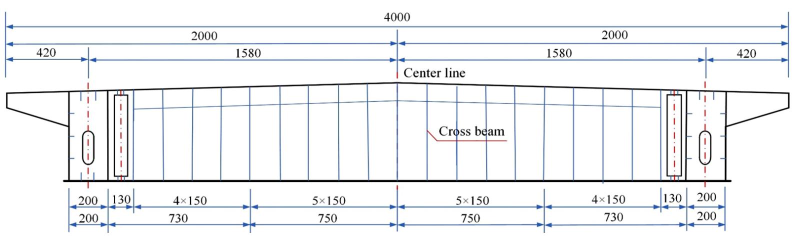


Fig. 2. Cross-sectional view of composite stiffening beam (unit: cm)

(3) Main cable and derrick

There are two main cables in the whole bridge, which are arranged in space. Each main cable consists of 37 strands of hexagonal prefabricated parallel steel wire, and each strand of prefabricated parallel steel wire consists of 127 high-strength galvanized steel wires with a diameter of Φ5.1 mm. The standard strength of main cable steel wire is 1670 MPa, and the designed elastic modulus is $2.0 \times 10^5$ MPa. According to the mechanical characteristics, they are divided into two specifications: $\varphi 7 \times 55$ and $\varphi 7 \times 91$. The southern half span is FS1~FS10 and the northern half span is FN1~FN10. The mid-span is MS1~M15~FN1, and the layout of the south bank suspenders is shown in Fig. 3.

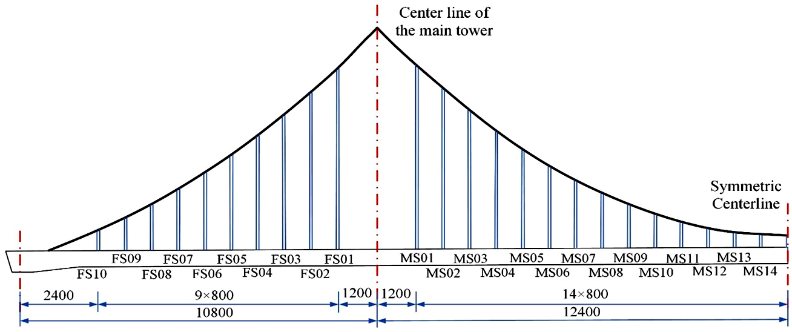


Fig. 3. Layout of south bank derrick (unit: cm)

# 3. Establishment of finite element analysis model

Establishing finite element model by Midas/Civil. The bottom consolidation boundary condition is adopted for the bridge tower. The boundary constraint of main girder is realized by general support. Rigid master-slave constraints are used to connect the anchor point of the main cable, the main cable at the main cable saddle and the connection between the suspender and the stiffening beam. The main cable is consolidated with the stiffened beam. The stiffened beam is a floating system and is not consolidated or supported with the tower beam. The whole bridge is divided into 2164 units and 1980 nodes. There are 104 main cable units and 98 suspender units, all of which are non-bending members, using cable units and truss units respectively. The main girder and bridge tower are flexural and compressive structures, and beam elements are selected. The finite element model is shown in Fig. 4.

Fig. 4. Finite element model of self-anchored suspension bridge

# 4. Analysis of structural static characteristics of the damage state

Suspension bridge belongs to high-order statically indeterminate structure, and its main components, steel-concrete stiffening beam and concrete pylon, will inevitably cause structural stiffness changes after being damaged, thus changing the structural stress form. Therefore, it is necessary to analyze the static characteristics of the damaged structure by assuming damage in the finite element model based on the static analysis of the nondestructive structure, so as to understand the corresponding static response of the bridge after a specific damage, which is conducive to the study of the applicability of the damage identification method.

In the finite element model, the damage can be simulated by reducing the stiffness. It is assumed that the damaged structure is moderately damaged, and the bending stiffness of the damaged position is reduced by 20%. For structural damage location and static analysis load, each damage condition is determined to enhance the comparison effect, as shown in Table 1. Under all working conditions, the analysis objects are still symmetrically selected unilateral main girder and south bridge tower, and the variable and its percentage in the analysis results are relative to the lossless structure.

Table 1. Damage location and damage condition

| **Static load** | **Mid-span 1/2 span test load** | | | | | |
|---|---|---|---|---|---|---|
| Damage condition | S1-1 | S1-2 | S1-3 | S1-4 | S1-5 | S1-6 |
| Damage location | Integral steel girder | M1 section | M2 section | M3 section | F2 section | Bridge tower as a whole |
| Static load | Mid span 1/4 span test load | | | | | |
| Damage condition | S2-1 | S2-2 | S2-3 | S2-4 | S2-5 | |
| Damage location | Integral steel girder | M1 section | M2 section | M3 section | F2 section | |
| Static load | Side span and middle span test load | | | | | |
| Damage condition | S3-1 | S3-2 | S3-3 | S3-4 | S3-5 | |
| Damage location | Integral steel girder | F2 section | F1 section | M4 section | M1 section | |

Under the action of integral damage conditions S1-1, S2-1 and S3-1, the deflection and bending moment of the stiffening beam are shown in Fig. 5 and Fig. 6. After the overall stiffness of the stiffening beam is reduced, the deflection of the 100 m area near the load position will further increase, with an added value of nearly 2 cm, which is about 20% of the original deflection value, while the deflection of the rest will decrease. On the contrary, the bending moment of the main tie beam decreases in a certain area under the action of load, while the distribution of lossless bending moment in other positions is alternately increased or decreased. It can be seen that after the stiffness of the steel beam changes, the internal force of the main beam will be redistributed, thus affecting its vertical deformation.

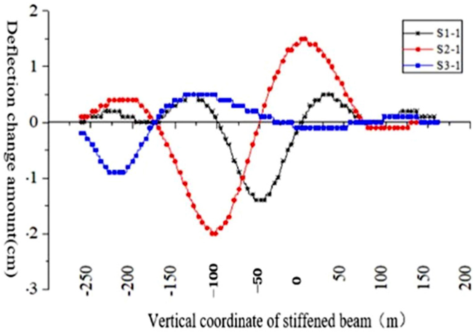


Fig. 5. Deflection variation of stiffened beam under overall damage condition

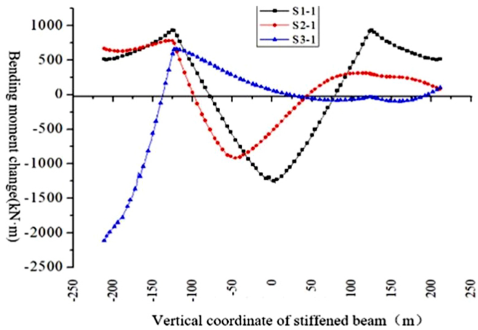


Fig. 6. Variation of bending moment of stiffened beam under overall damage condition

The damage of the main girder will have a great influence on the suspender cable force, causing the suspender force to redistribute, as shown in Fig. 7. The overall horizontal displacement change of the bridge tower is shown in Fig. 8. The overall damage of the main girder and the bridge tower will increase the longitudinal horizontal displacement of the bridge tower under the experimental load, and the increase of the horizontal displacement is close to ±0.15 cm, which shows that the horizontal displacement of the bridge tower is greatly affected by the stiffness of the main girder.

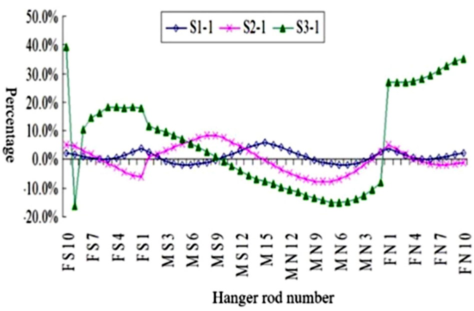


Fig. 7. Percentage of change of suspender cable force

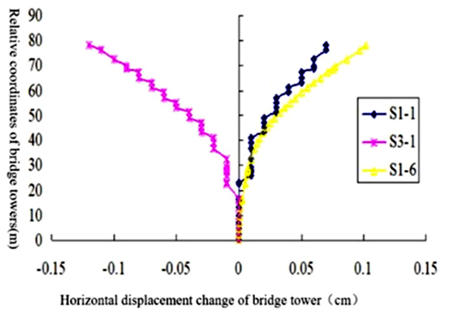


Fig. 8. Overall horizontal displacement change of bridge tower

Compared with the overall damage analysis, the deflection variation of the main girder under each test load is shown in Fig. 9 10 11. In the figure, in order not to make the damage condition with small relative variation be annihilated, the damage condition is appropriately amplified by integer times according to the principle of unified peak order of magnitude.

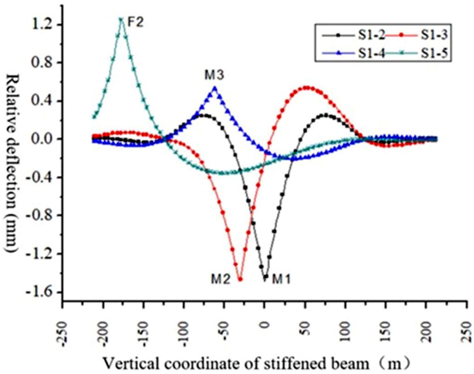


Fig. 9. Deflection of main girder partially damaged by 1/2 mid-span load variable quantity

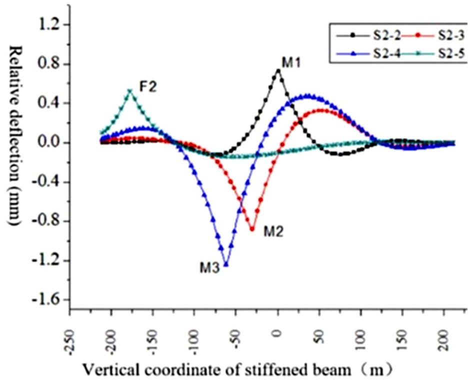


Fig. 10. Variation of deflection of main girder due to local damage of mid-span 1/4 span load

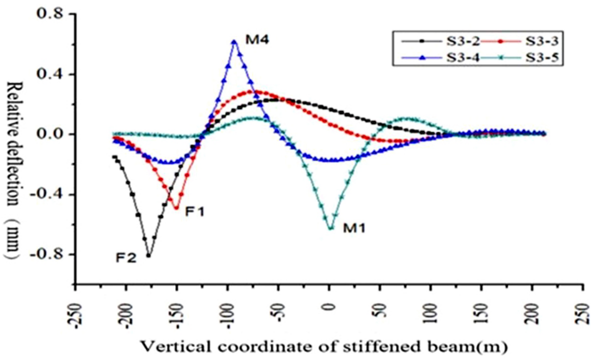


Fig. 11. Change of deflection of main beam with side span 1/2 span load

From Fig. 9 to Fig. 11, it can be seen that when static load is applied in the middle, quarter and side span of the main span, corresponding to the local damage of each main beam, no matter how far the damage position is from the load, the deflection variable of the main tie beam will have a significant peak at the damage point, which indicates the existence of the damage.

For the structural internal force change caused by local damage, the suspender cable force is taken as an example to illustrate. Under the action of local damage conditions, the cable force of the suspender changes as shown in Fig. 12–17, in which the magnitude of change of some damage points is greater than that of other positions, so it is expressed separately.

Through the above static damage analysis, we can know that the internal force and displacement will change significantly when the structure is damaged as a whole, and it is easy to identify by the deflection of the main tie beam and the cable force of the suspender. However, when the structure is only damaged locally, the deflection of the main tie beam and the variation of the cable force of the suspender will reflect obvious peaks at the damage position under various damage conditions, but if the peaks are not close to the load point, their absolute values are small.

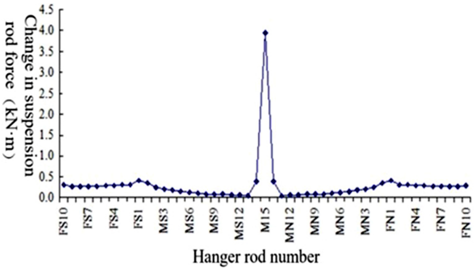


Fig. 12. S1-2 Variation of derrick force under damage condition

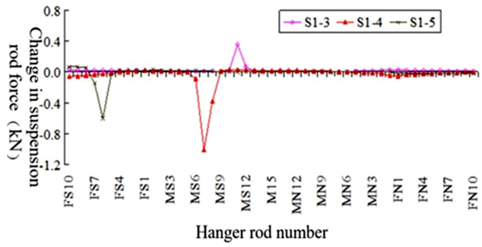


Fig. 13. S1-3~S1-5 Variation of boom force under damage condition

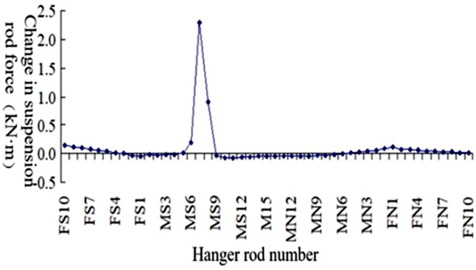


Fig. 14. S2-4 Variation of boom force under damage condition

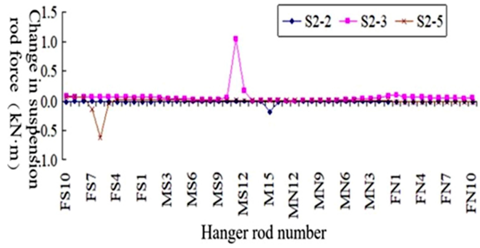


Fig. 15. Variation of damage suspender force at 1/4 non-loading point across load

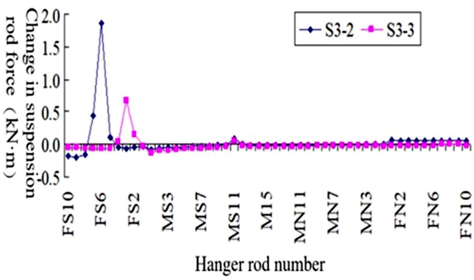


Fig. 16. Variation of suspender force under S3-2 and S3-3 damage conditions

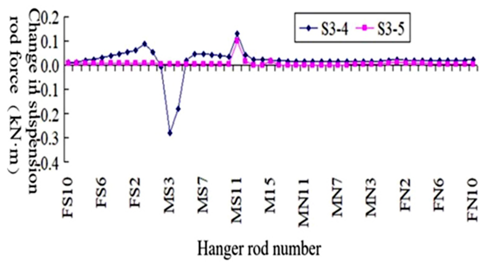


Fig. 17. Variation of suspender force under S3-4 and S3-5 damage conditions

# 5. Analysis of damage state stiffening beam dynamic response

In the state of structural damage, the change of static analysis results has been shown above, but the specific performance of the inherent dynamic characteristics of the structure that will affect the seismic and wind-resistant characteristics of the structure and the dynamic response of the moving vehicle load after damage needs further analysis.

The natural vibration characteristics of the whole structure and the response of the main tie beam of the 300 kN test vehicle under the action of moving at the design speed of 80 km/h are analyzed. The damage situation is set as three dynamic damage conditions: stiffening beam, integral damage of bridge tower and damage of M1 section in mid-span, and the damage degree is still 20% reduction of section stiffness to simulate.

The natural frequency will change after structural damage, in which the frequency change value caused by the overall damage of the main girder is greater than the corresponding value of the single damage of the main girder and the overall damage of the bridge tower in the table in most modes of the first ten orders, and the maximum value of –0.054 Hz appears in the sixth order mode. According to the matrix iterative solution of dynamic characteristics, it can be known that the natural vibration frequency is obtained from the mode matrix, and the change of frequency can indirectly indicate that the structural mode obtained by the final iteration has changed.

For the moving vehicle load, the time history analysis results of the bending moment and deflection of the damaged structure at the middle of the main span main tie beam are shown in Fig. 18–23.

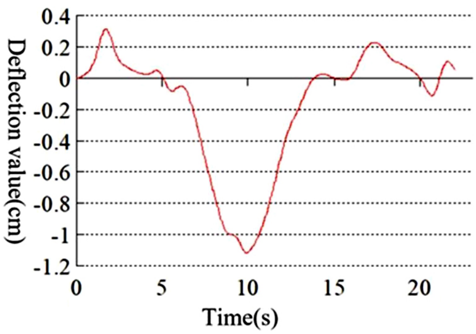


Fig. 18. Time-history diagram of deflection at M1 when the whole stiffened beam is damaged

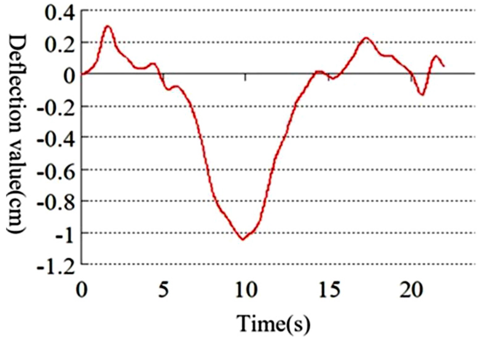


Fig. 19. Time-history diagram of bending moment at M1 when the whole stiffening beam is damaged

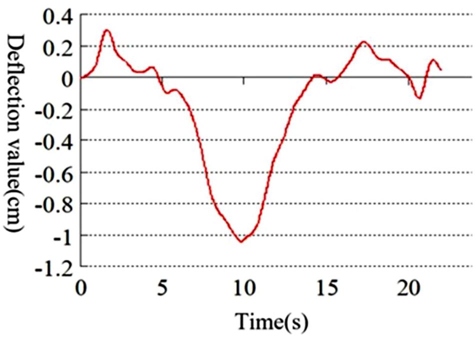


Fig. 20. Time-history diagram of deflection at M1 when the whole bridge tower is damaged

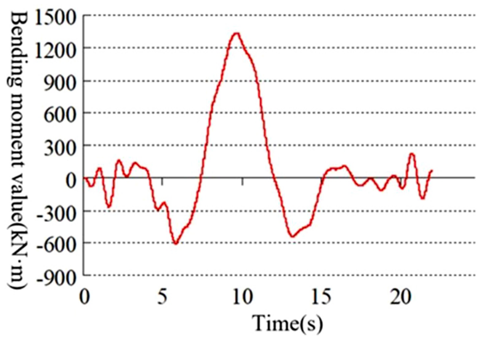


Fig. 21. Time-history diagram of bending moment at M1 when the whole bridge tower is damaged

From Fig. 18 to Fig. 23, it can be seen that the dynamic response history of intact structures is basically the same as that of structures with global and local damage. However, the changes of the peak mid-span response of the main tie beam under each damage are shown in Table 2.

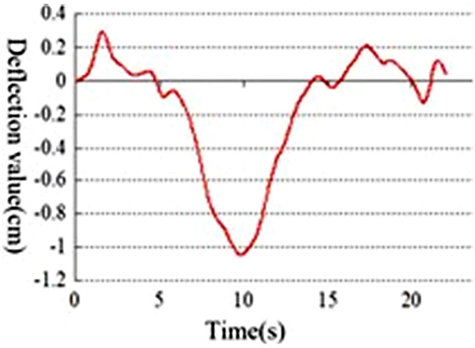


Fig. 22. Time-history diagram of deflection when M1 section is damaged

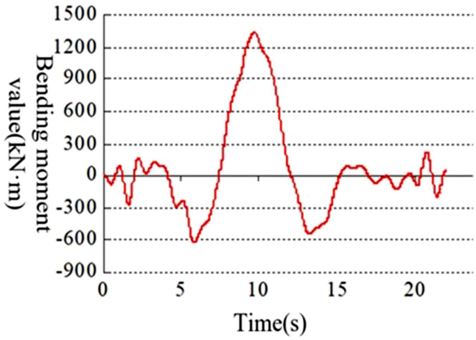


Fig. 23. Time-history diagram of bending moment when M1 section is damaged

Compared with the corresponding deflection moment value under the static load of a single vehicle, the static and dynamic changes under the overall damage are quite different, and the absolute value of the maximum difference rate is 38%.

Table 2. Damage dynamic response variables

| Damage location | Deflection (cm) | | Difference rate | Bending moment (kN·m) | | Difference rate |
|---|---|---|---|---|---|---|
| | Single vehicle static load | Single vehicle dynamic load | | Single vehicle static load | Single vehicle dynamic load | |
| Damage of main girder | 0.76 | 0.86 | 13% | –83.54 | –53.29 | –36% |
| Bridge tower damage | 0.21 | 0.13 | –38% | 17.3 | 12.26 | –29% |
| M1 section damage | 0.1 | 0.11 | 10% | 5.33 | 6.21 | 17% |

# 6. Analysis of boom rod influence

As the main load-bearing component of suspension bridge, suspenders are exposed to natural environment for a long time. If the protection fails, they are prone to corrosion and wire breakage under high tensile stress. Therefore, it is necessary to analyze and understand the static and dynamic effects of wire breakage on the structure. In order to make the analysis extensive, the following analysis shows the broken wire suspenders in both the main span and the side span. According to the structural symmetry, MS1 side suspender and M15 middle suspender are the main spans, and FS6 middle suspender in the south span is selected as the main analysis suspender for the side spans.

For the analysis load, because the broken wire of the boom is most likely to occur under the corresponding moving load that produces the maximum boom force in the normal operation stage, the static analysis of the broken wire of the boom can make the analysis result more reasonable and conform to the actual state. At the same time, considering that the magnitude and arrangement of the moving load corresponding to the maximum cable force of each suspender in the same span are basically the same, but there are differences between different spans, only the corresponding values of M15 suspender and FS6 suspender are set for analyzing the moving load.

## 6.1. Broken wire state of single derrick

This paper analyzes the wire breakage of suspenders MS1, M15 and FS6 alone, in which suspenders MS1 and M15 of the main span are assumed to be broken under the mid-span analysis load, and the other analysis load is not considered. However, the broken wire of the side span FS6 suspender is caused by its side span analysis load, so it is only used for static analysis. In the analysis, wire breakage is simulated by reducing the cross-sectional area a of the suspender. After wire breakage, the suspender area is expressed as $\beta A$, where $\beta$ is the wire breakage coefficient. In the analysis, the values are 0.8 and 0 according to the conditions of moderate damage and complete failure.

In the case of two kinds of broken wires, the variation of suspender cable force is shown in Fig. 24 and Fig. 25. As can be seen from the figure, when 20% of the wire of the boom is broken, the cable force of the boom will be reduced by about 6%, and most of the reduction will be added to its left and right adjacent booms. Due to the adjacent influence principle, the cable force of the other booms will be almost unaffected. At the same time, the variation law of the cable force of the suspenders is in direct proportion to the degree of damage. After 100% wire breakage of the suspenders, the cable force of the damaged suspenders drops to zero, and the increase of the cable force of the adjacent suspenders reaches an extreme value, of which the maximum increase is 130 kN, which occurs in the suspenders of MS14 and MN14. The change of cable force under the dead weight of these two suspenders is also the largest, increasing to 3114.2 kN, which makes the cable force of load combination 3573.2 kN, and the safety factor is greatly reduced, which is prone to chain cable breaking reaction.

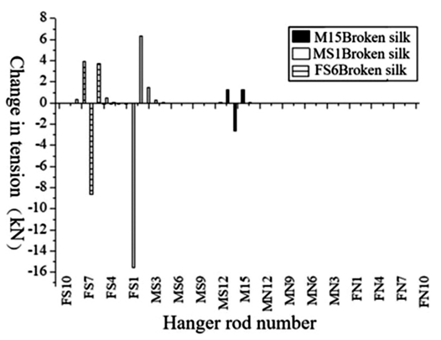


Fig. 24. Variation of cable force under 20% damage of broken wire hanger

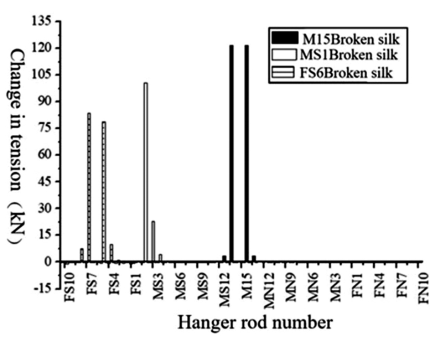


Fig. 25. Variation of cable force under complete failure of broken wire hanger

However, the change of suspender force after wire breakage in different degrees will also have an impact on the bending moment and deflection of the main tie beam as shown in Fig. 26 and Fig. 27.

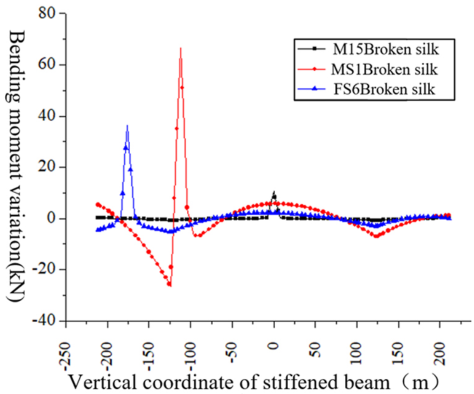


Fig. 26. Variation of bending moment of main tie beam under 20% damage of broken wire hanger

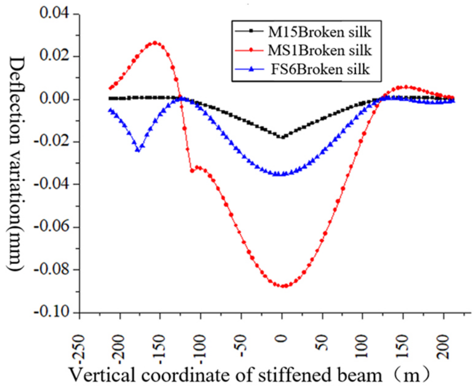


Fig. 27. Deflection change of main tie beam under 20% damage of broken wire hanger

From Fig. 26 to Fig. 29, it can be seen that the bending moment of the main tie beam only changes obviously in the area near the damage of the suspender, which is caused by the change of the cable force of the suspender, and the maximum change value of the bending moment can reach about 1000 kN·m after the suspender loses its function, which has an additional stress of about 2 MPa for the main tie beam.

For the deflection of the main tie beam, the maximum change value under the damage of each suspender is 1.5 mm, and all of them appear in the middle of the main span. This is mainly due to the large deflection value at this position, which makes the deflection change at the

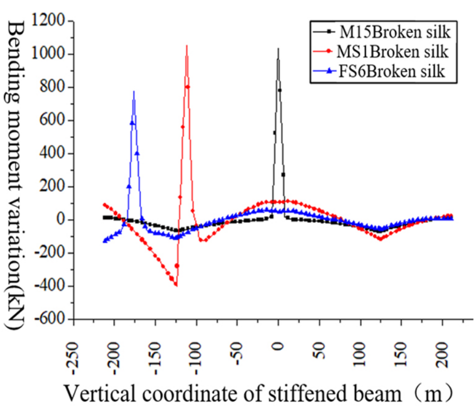


Fig. 28. Main tie beam under complete failure of broken wire hanger variation of bending moment

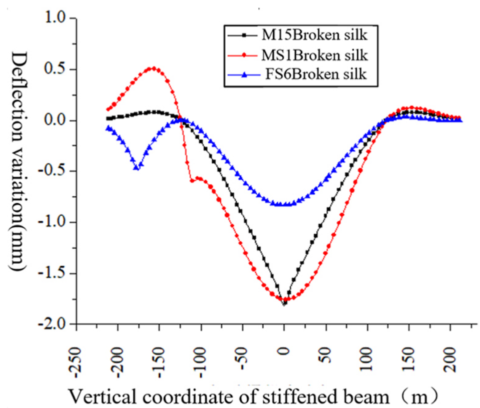


Fig. 29. Main tie beam under complete failure of broken wire hanger deflection change

damage position ignored. When compared with the deflection change, the maximum relative deflection change is at the damaged suspender, and its value is nearly 45%, as shown in Fig. 30.

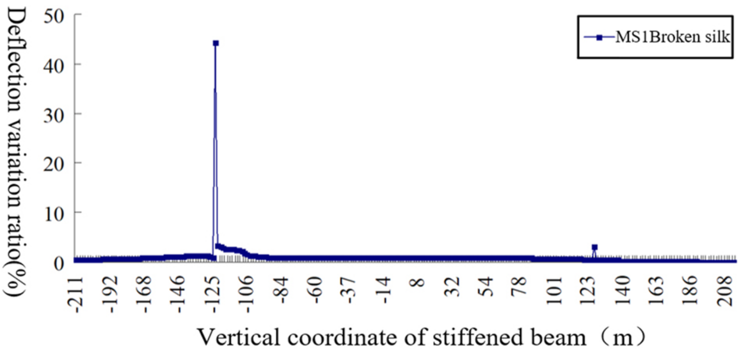


Fig. 30. Percentage change of deflection of main tie beam under complete failure of suspender

## 6.2. Broken wire state of multiple suspenders

Based on the damage analysis of individual suspenders, in order to further understand the influence of broken wires on the structure, two broken wires suspenders, MS7 and FS3, are added at the quarter of the main span, and the combined damage analysis of multiple broken wires suspenders is carried out at the same time. The combination methods are as follows:

- Combination 1: M15 suspender +MS7 suspender+MS1 suspender with broken wire by 20%.
- Combination 2: FS6 suspender +FS3 suspender broken wire by 20%.
- Combination 3: All selected suspenders are damaged by 20%.

Considering that the changes of the bending moment and deflection of the main tie beam structure are relatively small after the broken wire, and are mainly influenced by the changes of the suspender force, in the combination analysis of the broken wire of the suspender, the changes of the suspender force are mainly analyzed, as shown in Fig. 31–33.

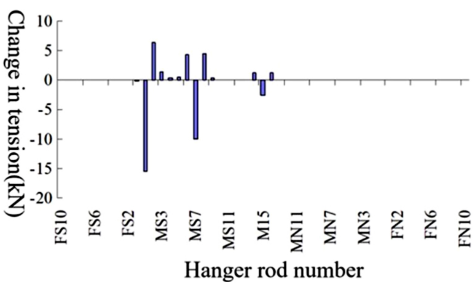


Fig. 31. Variation of lower boom force in combination 1

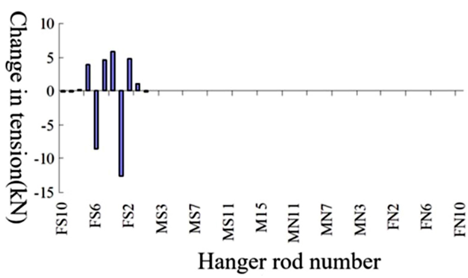


Fig. 32. Variation of lower boom force in combination 2

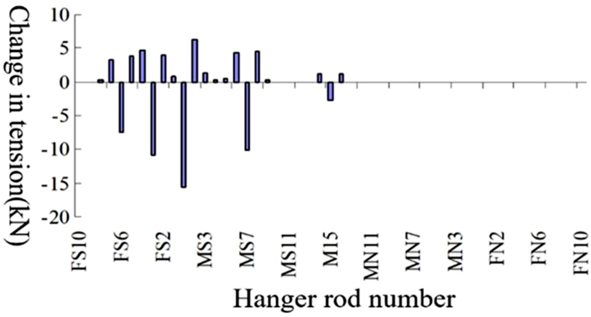


Fig. 33. Change of lower boom force in combination 3

From combination 1 to combination 3, it can be seen that the law of cable force change is the same as that of single suspender damage when multiple suspenders are damaged in the same span or different spans, and the obvious cable force change is at the damage and adjacent suspenders. At the same time, the value of suspender force change is very close to that of the same suspender damage, which shows that there is basically no effect on suspender force between different damaged suspenders.

## 7. Conclusions

The static load response analysis and structural dynamic characteristics analysis are carried out, and then the static and dynamic responses of the stiffened beam, the bridge tower damaged and the suspender broken wire are compared and analyzed respectively, so as to understand the changing characteristics of internal force and displacement of the structure after damage, and the following main conclusions are obtained:

– When the stiffening beam or bridge tower is damaged, the bending moment and deflection of the main tie beam, the horizontal displacement of the bridge tower and the cable force of the suspenders will change greatly under the overall damage, and the cable force of the side suspenders can change by 40%.
– When the wire of the suspender is broken under the most unfavorable moving load, the deformation and bending moment of the main girder are mainly reflected in the damaged suspender. Among them, the cable force of suspenders damaged by multiple suspenders also applies to this law, and there is no obvious influence between damaged suspenders.
– After the suspenders fail completely, the deformation and internal force of the bridge will increase greatly, and the cable force of the adjacent suspenders will increase by 50% at most under the dead weight and the maximum cable force moving load, which will most likely cause the chain fracture of the adjacent suspenders. Lead to the destruction of the bridge.
– The internal force and deformation caused by the same static and dynamic load and the inherent dynamic characteristics of the structure will change correspondingly when different damages occur to the structure, but the change is small for the moderate damage of 20%.

## Acknowledgements

The research was supported by National Natural Science Foundation of China (U2239252) and Key R&D Program of Heilongjiang Province (Grant No. GA22C001)

## References

[1] L. Jianhui, L. Aiqun, and Q.F. Maria, "Sensitivity and reliability analysis of a self-anchored suspension bridge", *Journal of Bridge Engineering*, vol. 18, no. 8, pp. 703–711, 2013, doi: 10.1061/(ASCE)BE.1943-5592.0000424.

[2] W. Zhiyong, G. Guohe, et al., "Investigation on cracking performance of UHPC overlaid concrete deck at hogging moment zone of steel-concrete composite girders", *Archives of Civil Engineering*, vol. 69, no. 4, pp. 445–457, 2023, doi: 10.24425/ace.2023.147669.

[3] X. Fuyou, Z. Mingjie, W. Lei, and Z. Zhe, "Self-anchored suspension bridges in China", *Practice Periodical on Structural Design and Construction*, vol. 22, no. 1, 2017, doi: 10.1061/(ASCE)SC.1943-5576.0000304.

[4] L. Yan, Z. Chengxin, L. Jun, et al., "Flexural performances of steel–concrete composite section of self-anchored suspension bridge: Experimental and theoretical research", *Structures*, vol. 56, 2023, doi: 10.1016/j.istruc.2023.105047.

[5] Wang, Xiaoming, W. Huan, S. Yuan, et al., "Process-independent construction stage analysis of self-anchored suspension bridges", *Automation in Construction*, vol. 117, art. no. 103227, 2020, doi: 10.1016/j.autcon.2020.103227.

[6] A. Yonghui, E. Chatzi, S. Sunghan, et al., "Recent progress and future trends on damage identification methods for bridge structures", *Structural Control and Health Monitoring*, vol. 26, no. 10, art. no. e2416, 2019, doi: 10.1002/stc.2416.

[7] Q. Wenting, M. Biao, L. Qiangwei, et al., "Computer vision-based bridge damage detection using deep convolutional networks with expectation maximum attention module", *Sensors*, vol. 21, no. 3, art. no. 824, 2021, doi: 10.3390/s21030824.

[8] W. Guangrun, Q. Wenliang, and W. Tianyu, "Nonlinear dynamic analysis of the self-anchored suspension bridge subjected to sudden breakage of a hanger", *Engineering Failure Analysis*, vol. 97, pp. 701–717, 2019, doi: 10.1016/j.engfailanal.2019.01.028.

[9] A.C. Neves, I. González, J. Leander, and R. Karoumi, "Structural health monitoring of bridges: a model-free ANN-based approach to damage detection", *Journal of Civil Structural Health Monitoring*, vol. 7, pp. 689–702, 2017, doi: 10.1007/s13349-017-0252-5.

[10] N. Jianguo, T. Muxuan, F. Jiansheng, "Research on cable anchorage systems for self-anchored suspension bridges with steel box girders", *Journal of Bridge Engineering*, vol. 16, no. 5, pp. 633–643, 2011, doi: 10.1061/(ASCE)BE.1943-5592.0000190.

[11] Z. Yu, Z. Yongjun, W. Lingling, et al., "Experiment on the behavior of a self-anchored suspension and cable-stayed hybrid bridge during structural transformation", *KSCE Journal of Civil Engineering*, vol. 24, pp. 1821–1831, 2020, doi: 10.1007/s12205-020-0881-9.

[12] Z. Guangpan, L. Aiqun, L. Jianhui, and D. Maojun, "Structural health monitoring and time-dependent effects analysis of self-anchored suspension bridge with extra-wide concrete girder", *Applied Sciences*, vol. 8, no. 1, art. no. 115, 2018, doi: 10.3390/app8010115.

[13] C.R. Farrar and D.A. Jauregui, "Comparative study of damage identification algorithms applied to a bridge: I. Experiment", *Smart Materials and Structures*, vol. 7, no. 5, art. no. 704, 1998, doi: 10.1088/0964-1726/7/5/013.

[14] R.W. Wickramasinghe, P.D. Thambiratnam, and T.H.T. Chan, "Damage detection in a suspension bridge using modal flexibility method", *Engineering Failure Analysis*, vol. 107, art. no. 104194, 2020, doi: 10.1016/j.engfailanal.2019.104194.

[15] J.C. Weinstein, M. Sanayei, and B.R. Brenner, "Bridge damage identification using artificial neural networks", *Journal of Bridge Engineering*, vol. 23, no. 11, art. no. 04018084, 2018, doi: 10.1061/(ASCE)BE.1943-5592.0001302.

[16] O. Huth, et al., "Damage identification using modal data: Experiences on a prestressed concrete bridge", *Journal of Structural Engineering*, vol. 131, no. 12, pp. 1898–1910, 2005, doi: 10.1061/(ASCE)0733-9445(2005)131:12(1898).

[17] A. Fernandez-Navamuel, et al., "Supervised deep learning with finite element simulations for damage identification in bridges", *Engineering Structures*, vol. 257, art. no. 114016, 2022, doi: 10.1016/j.engstruct.2022.114016.

[18] M.G. Masciotta, L.R. Ramos, et al., "A spectrum-driven damage identification technique: Application and validation through the numerical simulation of the Z24 Bridge", *Mechanical Systems and Signal Processing*, vol. 7071, pp. 578–600, 2016, doi: 10.1016/j.ymssp.2015.08.027.

Received: 2024-05-25, Revised: 2024-07-12